Using Artificial Neural Network (ANN) for Prediction of Climate Change Impacts on Jointed Plain Concrete Pavement

Mohammad Shafiee, Ph.D., P.Eng.
Research Officer
Construction Research Centre
National Research Council Canada

Omran Maadani, Ph.D.
Research Officer
Construction Research Centre
National Research Council Canada

Eslam Fahiem, MSc
Graduate Student
Carleton University

Paper prepared for the Innovations in Pavement Management,
Engineering and Technologies session of the 2021
TAC Conference & Exhibition

Abstract

Driven by human influence, Canada's climate has warmed and will warm further at a rate of double the global average. Climate change phenomenon, commonly known as 'global warming', is expected to cause irreversible temperature rise as well as other environmental anomalies that could affect transportation infrastructures. With continued growth in greenhouse gas (GHG) emissions in future, rising temperatures will have consequences on the short and long-term performance of the Jointed Plain Concrete Pavement (JPCP) systems. In this study, climate change impact on a typical JPCP structure was modeled using Pavement ME Design (PMED) software. The PMED modeling results were fed into a two-layer feed-forward network with sigmoid hidden neurons and linear output neurons. Results of this study indicated that the developed ANN models are effective and capable of accurately predicting the potential and relative impact of climate change on JPCP.

Introduction

The interaction of the ambient temperature, solar radiation, cloud cover, precipitation, and depth of water table with the pavement materials and the traffic loading is usually known to be a complicated phenomenon. Particularly, transverse cracking in JPCPs is extremely sensitive to climate condition. Many studies have confirmed that when top of the slab is warmer than the bottom of the slab, normally during daytime, repeated traffic loading can initiate bottom-up transverse cracks which can become visible on the surface over time. However, when bottom of the slab is warmer than the top of the slab, normally during nighttime, top-down transverse cracks are often initiated under traffic load repetitions [1]. It is interesting to note that, JPCP paving in hot days may create permanent built-in temperature gradient which is even more favorable for future top-down cracks. In fact, in addition to the heat supplied from intense solar radiation during hot days, the fresh Portland Cement Concrete (PCC) also generates hydration heat during hardening process. As a result, top of the slab remains warmer than the bottom during solidification period and a positive temperature gradient or a Zero-Stress Temperature (ZST) gradient gets locked into the PCC. Consequently, upward curling with increased stress at top of the slab occur anytime that in-service temperature gradient drops below ZST [2].

Previous studies have shown that reducing the risks of climate change on pavement performance requires scaled-up design tools based on adequate Mechanistic- Empirical model. Owing to the Enhanced Integrated Climatic Model (EICM) within Pavement ME Design (PMED) software, which can simulate the material behavior due to climatic variations, pavement designers can better predict the relative effect of climate change on JPCPs. With direct control over many climatic inputs of the project, designer have been able to quantify the structural performance of JPCP by incorporating credible quantitative estimates of future climate change. However, the extensive amount of detailed material, foundational, traffic and environmental inputs presents a challenge for many small road agencies wishing to implement the PMED. Nevertheless, by virtue of advance computing systems such as Artificial Neural Network (ANN) techniques, broadly developed after human brain's neural networks, the patterns of climate change's impacts can be simulated.

Previous case study in Minnesota showed that ANN is a good candidate to predict flexible pavement's layer moduli in the future under climate change. Using this approach, researchers observed that their developed ANNs were capable of learning the Falling Weight Deflectometer (FWD) measurements and corresponding influential inputs [3]. In another study conducted at University of Toronto, machine learning algorithms were used to predict the effect of climate change on damage accumulation for flexible pavements. Using this method, researchers captured the difference between maintenance policies before and after climate change as well as the corresponding added costs [4]. Elsewhere, machine learning techniques were used to optimize pavement management strategies for a diverse range of possible future scenarios [5]. Current paper investigates an innovative approach using trained ANN to predict climate change effect on the JPCP performance for a typical cold region pavement in Winnipeg, Manitoba.

Methodology

As illustrated in Figure 1, ANN was employed in this study with the objective to predict the slab cracking and joint faulting under future climate change. First, series of simulations were carried out using the AASHTOWare Pavement ME Design (PMED). Later, ANN was trained and evaluated using outputs from a large number of PMED runs with projected climate data. Climate change data was obtained from the outputs of the Canadian Regional Climate Model (CanRCM4) [6] developed by the Canadian Centre for

Climate Modelling and Analysis (CCCma) under Representative Concentration Pathway (RCP) 8.5. This high emission scenario reflects the most likely 'business as usual' emission trajectory. Climate data consisted of mean hourly temperatures, wind speed, percent sunshine, precipitation, relative humidity and water table depth. As shown in Table 1, one baseline and three future scenarios for the City of Winnipeg, Manitoba, were set up to investigate the relative impact of climate change on JPCP performance. As depicted, Mean Annual Air Temperature (MAAT), Mean Annual Precipitation (MAP), and estimated ZSTs are all expected to rise in view of projected changes in climate. By definition, the ZST is illustrates the average temperature in the PCC slab at the time the concrete sets and is empirically calculated based on the mean monthly temperature of the month of construction.

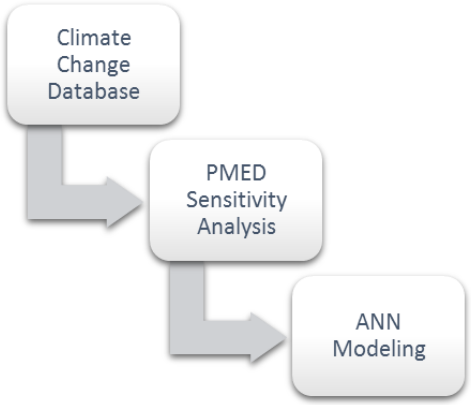

Figure 1- Modeling the Climate Change Impact on Pavement Performance

Table 1- Selected Climate Change Scenarios

Scenario	Analysis Period	Mean Annual Air Temperature (℃)	Mean Annual Precipitation (mm)	Estimated ZST (℃)
Baseline	1995-2020	6.31	597.66	37.6
Short-term future	2025-2050	8.27	617.22	38.5
Medium-term future	2050-2075	10.56	636.02	41.6
Long-term future	2075-2100	12.79	701.80	44.4

A four-lane unreinforced cast-in-place JPCP with doweled transverse joints and tied shoulders was analyzed in this study. The pavement design life was assumed to be 25 years for the purpose of this impact study. A series of sensitivity analysis were conducted by varying five key input parameters including Annual Average Daily Truck Traffic (AADTT), the thicknesses for Portland Cement Concrete (PCC) and Granular Base Course (GBC), and the resilient modulus for GBC and subgrade (SG), as shown

in Table 2. Other controlling variables were held constant as depicted in Table 3 [7]. It is however important to note that the abovementioned conditions are typical for Level-3 (default) analysis. Overall, a total of 972 case studies were modeled using the latest release of the AASHTOWare PMED, version 2.6.0.

Table 2- Different Sensitivity Analysis Cases

Variable	Range of Values
AADTT	5000, 7500 and 10000
PCC Thickness (mm)	170, 180 and 190
GBC Thickness (mm)	150, 200 and 250
GBC Resilient Modulus (MPa)	150, 200 and 250
SG Resilient Modulus (MPa)	30, 50 and 70

Table 3- Design input properties for AASHTOWare PMED

Design Feature	Input Parameter	Value
PCC Properties	28-day Modulus of Rupture (MPa)	5.6
	Coefficient of Thermal Expansion (mm/mm °C x 10^{-6})	7.8
	Heat Capacity (joule/kg-Kelvin)	1172.0
	Unit Weight (kg/m^3)	2320.0
	Thermal Conductivity (watt/meter-Kelvin)	2.16
JPCP Design	Permanent curl/warp effective temperature difference (°C)	-5.6
	Dowel diameter (mm)	32
	Erodibility Index	5
Pavement Performance	Initial IRI (m/km)	1.5
	Reliability	90%

In an attempt to reproduce and model climate change impact on performance trends, a set of input vectors inserted in one matrix and a set of associated target vectors inserted into another were defined for all cases. As part of the multidimensional mapping mechanism, two-layer feed-forward networks with sigmoid hidden neurons and linear output neurons were created accordingly. Figure 2 shows the schematic diagram of the ANN model implemented in this study. As can be seen, seven types of input variables were introduced in the models among which were the MAAT and MAP variables. Input layer holds neurons receiving inputs directly from outside the network, as shown in the figure. The input layer is followed by the hidden layer with fairly arbitrary number of hidden neurons and the so-called transfer function in the hidden layer is sigmoid by default. As can be seen in Figure 2, the next layer of the network is the output layer of linear neurons. It is worth noting that two separate models, each with one output neuron, were developed for faulting and cracking.

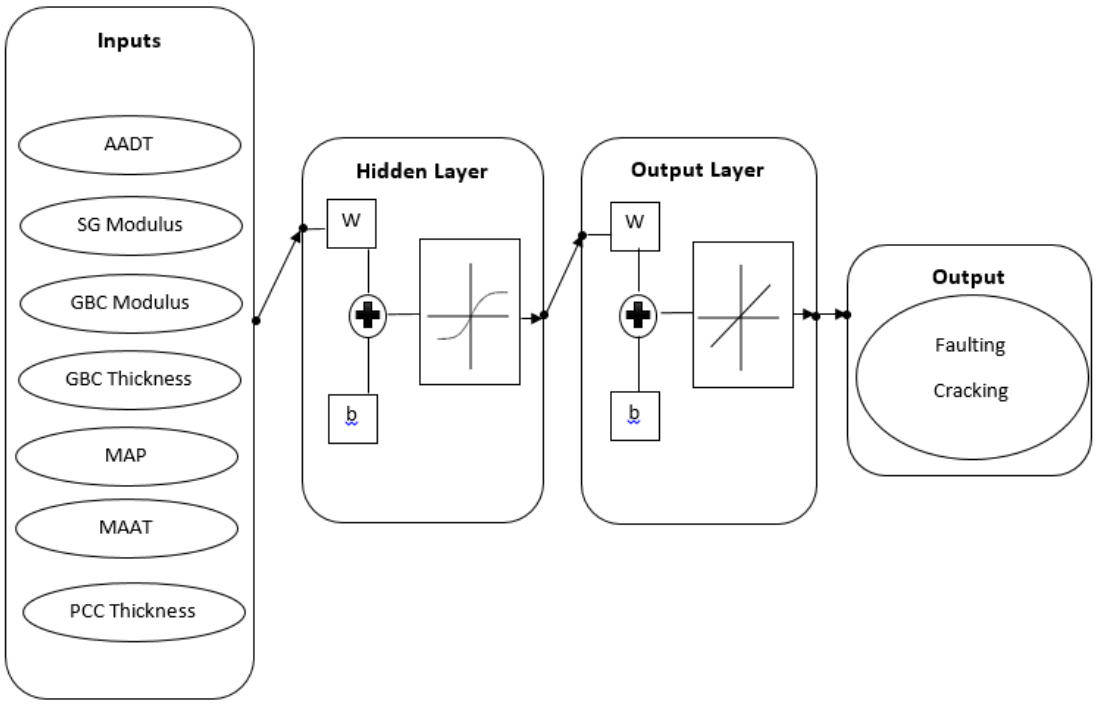

Figure 2- Diagram of the ANN modeling structure

Following the general workflow for a multilayer network, each group of dataset was first divided in three subsets. The first subset was used for training and included 70 percent of the entire data randomly selected in each group. Training subset is essential for computing the gradient and updating the network weights and biases. Subsequently, both the second and third subsets used for network validation and testing purposes, respectively, consisted of 15 percent of the entire data. When training, the error on the validation set is continuously checked. Basically, the validation error will normally decrease as long as the network is in the process of learning the targets, or more specifically, during the initial phase of training. However, as soon as the network begins to overfit the data, the error on the validation set typically begins to rise. Thus, the network weights and biases are set at the point where the validation

error is minimum. In this study, the default criteria for network training termination pertaining to the magnitude of the gradient of performance and the number of validation checks, was applied during the process. By default, training phase automatically stopped after six unsuccessful attempts to reduce the validation error or once the gradient magnitude became less than 1e-5. For this function approximation problem, Levenberg–Marquardt (L-M) backpropagation algorithm, which uses Jacobian calculations, was adopted to train the networks. This L-M algorithm, supported by MATLAB's built-in functions, was chosen as it is known to be the fastest and most efficient approach for training medium-sized networks with up to a few hundred weights. It is worth noting that due to the random sampling scheme, retraining may yield different results each time. In other words, each retraining session normally starts with different initial weights and biases. Also, the procedure of random data division results in loading different training, validation and testing datasets in each retraining session.

Results and Discussions

Figure 3 (a) and (b) show the faulting and cracking for all evaluated cases, respectively. As can be seen, warmer climate in future is generally expected to increase the risk of faulting. This can be partially attributed to the ZST's effect on the joint behavior. As stated in the MEPDG, lower ZST leads to the tighter joints over time because the joints open when the temperature within the slabs falls below the ZST. Therefore, increase in ZST may be associated with larger faulting over the life of the pavement. In fact, chances of higher ZSTs could be greater in view of climate change, as previously shown in Table 1.

However, climate change seems to be causing less fatigue cracking relative to the baseline scenario according to the examined cases. While a constant permanent curl/warp is present in the slab, effect of climate change on transitory curling and transitory warping is obviously responsible for such impacts. As per the MEPDG, climatic factors including solar radiation, cloud cover, precipitation, ambient temperature, and depth to water table can directly influence the temperature and moisture state in pavement and subgrade and eventually the critical stresses involved [1].

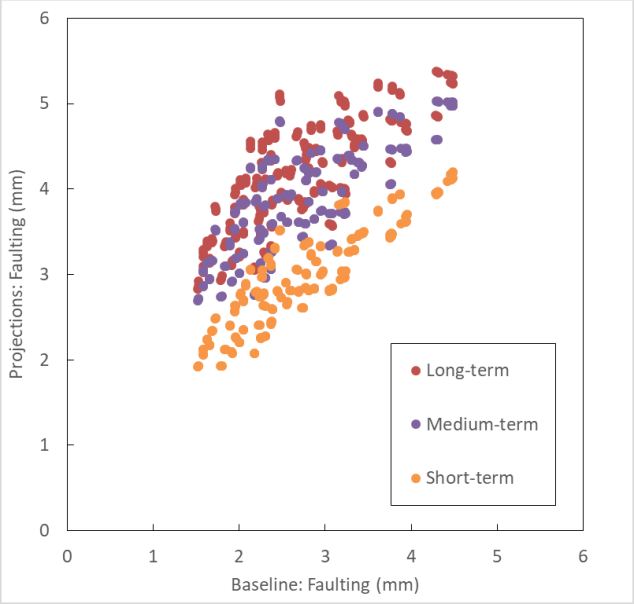

(a)

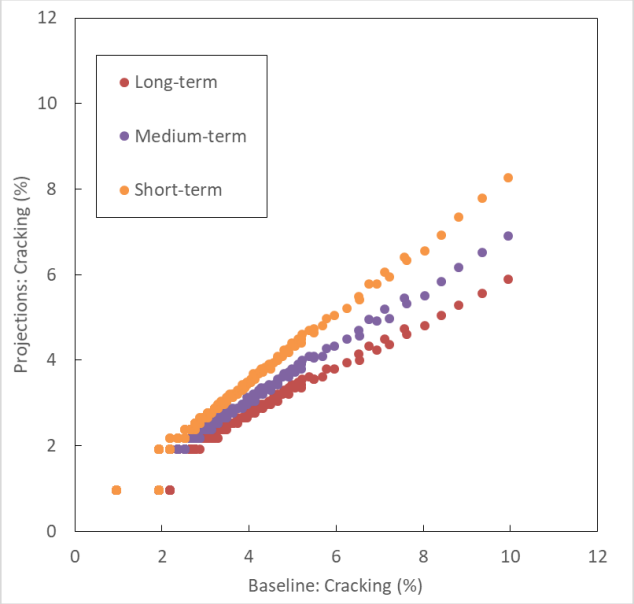

(b)

Figure 3- Comparison of PMED-predicted (a) faulting and (b) cracking distresses

Comparing the averaged distress values at different input levels also revealed the sensitivity of faulting and cracking to AADTT, concrete thickness, base thickness, base resilient modulus and subgrade resilient modulus. It is evident from Figure 4 that increasing the PCC slab thickness from 170 mm to 190 mm can decrease the cracking by almost 60.5% and increase the joint faulting by almost 7.6%. Hence, thicker PCC slabs make the JPCP less prone to cracking, but slightly more prone to faulting. According to the MEPDG, increasing the PCC slab thickness without corresponding increase in the dowel diameter will reduce the effective area of the bar relative to the slab thickness which will lead to higher risk of faulting. It is also clear from the figure that higher traffic load will cause further increase in both faulting and cracking distresses on average by 39.8% and 50.9%, respectively. Within the examined range of GBC properties, it was found that both faulting and cracking were more sensitive to the GBC thickness rather than the GBC resilient modulus. In terms of the GBC resilient modulus, results indicated that increasing the modulus from 150 MPa to 250 MPa can reduce the cracking by 11.6% and faulting by only 0.2%. On the other hand, increasing the subgrade modulus from 30 MPa to 70 MPa appeared to reduce the cracking and faulting by 45.4% and 20.9%, respectively.

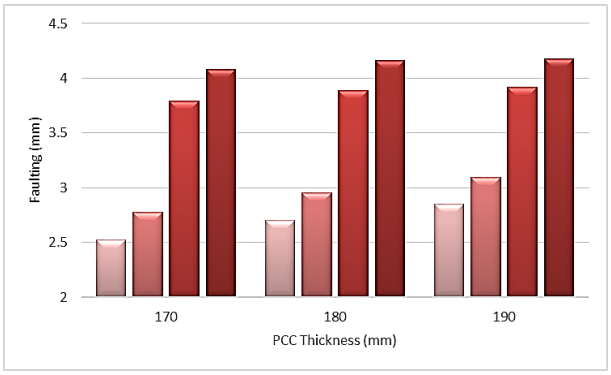
Faulting (mm)
4.5
4
3.5
3
2.5
2
170
180
190
PCC Thickness (mm)

(a)

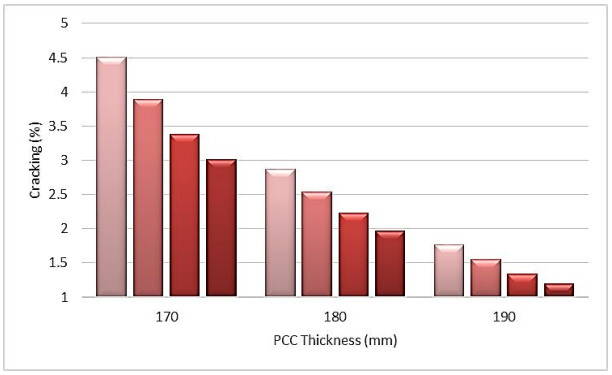
Cracking (%)
5
4.5
4
3.5
3
2.5
2
1.5
1
170
180
190
PCC Thickness (mm)

(b)

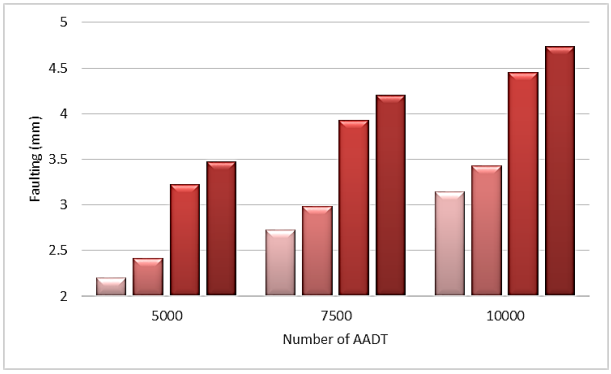
Faulting (mm)
5
4.5
4
3.5
3
2.5
2
5000
7500
10000
Number of AADT

(c)

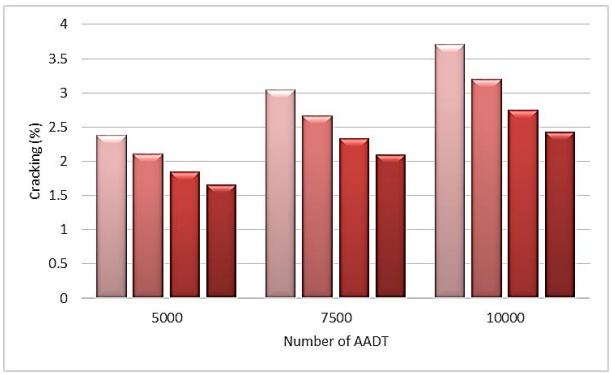
Cracking (%)
4
3.5
3
2.5
2
1.5
1
0.5
0
5000
7500
10000
Number of AADT

(d)

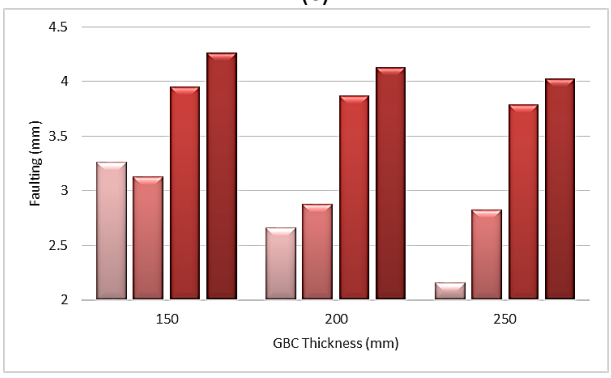
Faulting (mm)
4.5
4
3.5
3
2.5
2
150
200
250
GBC Thickness (mm)

(e)

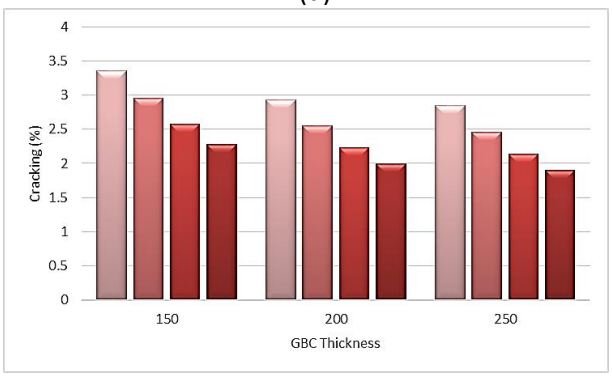
Cracking (%)
4
3.5
3
2.5
2
1.5
1
0.5
0
150
200
250
GBC Thickness

(f)

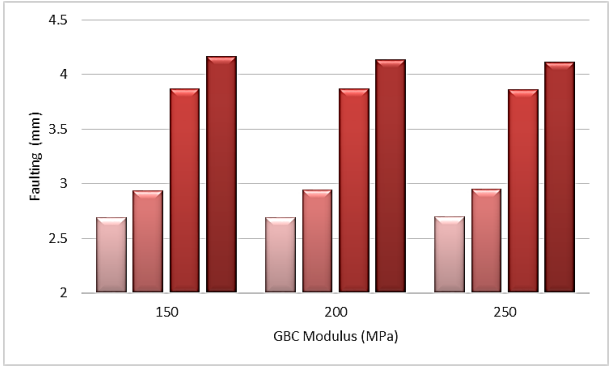
Faulting (mm)
4.5
4
3.5
3
2.5
2
150
200
250
GBC Modulus (MPa)

(g)

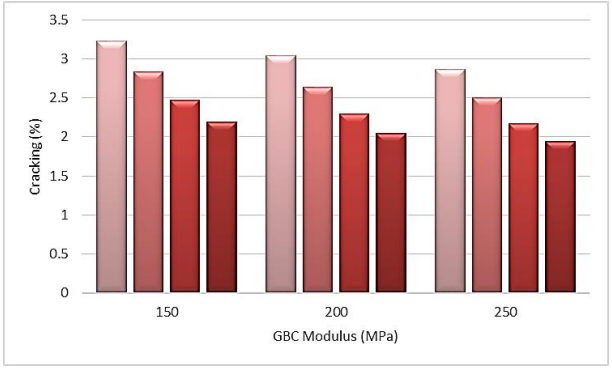
Cracking (%)
3.5
3
2.5
2
1.5
1
0.5
0
150
200
250
GBC Modulus (MPa)

(h)

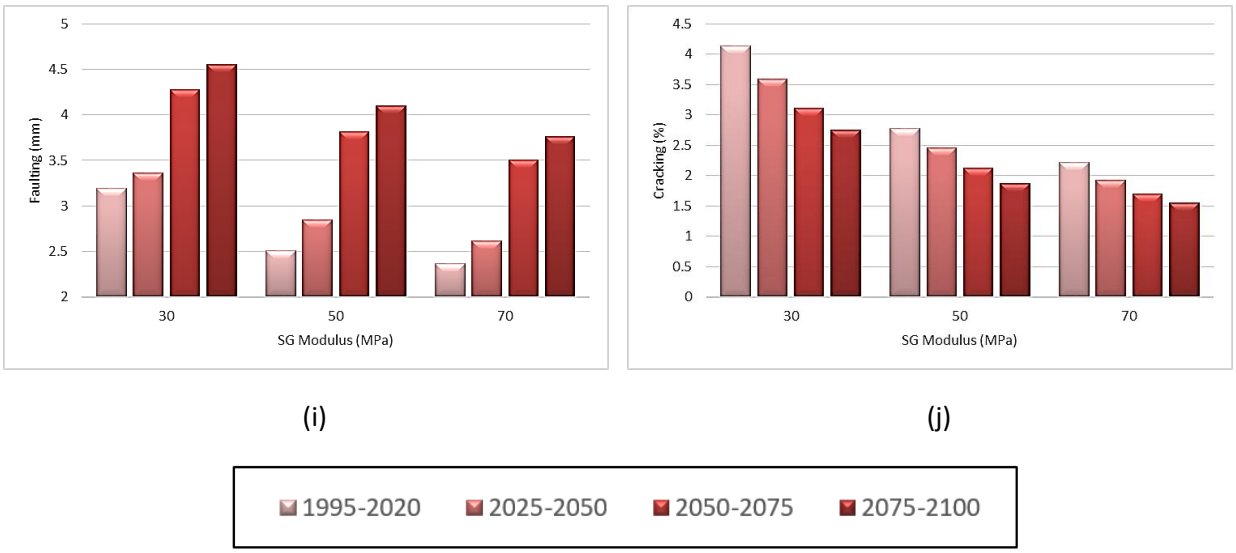

Figure 4- Sensitivity of PMED-predicted distresses to different design input levels

In the next part of the analysis, data was imported to the MATLAB's Deep Learning Toolbox [8] in order to create fitting functions. While developing the models, it was recognized that although more neurons in the hidden layer entail more computation time and higher potential for overfitting the data, they may enhance network's capability in case of complex problems. In other words, higher numbers of neurons in the hidden layer give the network more flexibility because the network has more parameters it can optimize. The number of hidden neurons was chosen to be 10 in this study and the resultant network performance was relatively stable. By definition, *mse* is determined as the mean sum of squares of errors between the network-predicted outputs (a_i) and the observed target data (t_i), as shown in Equation 1.

$$mse = \frac{1}{N}\sum_{i=1}^{N}(e_i)^2 = \frac{1}{N}\sum_{i=1}^{N}(t_i - a_i)^2 \qquad (1)$$

As with any neural network analysis, care was taken to avoid overfitting. Basically, the error becomes smaller after more epochs of training, nonetheless it might begin to rise on the validation data set once the overfitting occurs. That is, the network may start to memorize the training examples it has seen, rather than actually learn to generalize to new situations as they come. Reasonable performance levels were obtained considering that the final *mse* was found to be quite small. Reviewing learning curves of the developed model indicated that the validation and test curves were somewhat similar. Consequently, network overfitting did not seem to be a problem. Even though the test set error is not used during training, it is useful as a further check of the network generalization capability,

independently. Normally, if the error on the test set had reached a minimum at a significantly different iteration number than the validation set error, it could indicate that a poor division of the data set might have occurred. Table 4 shows the *mse* and *R-squared* metrics obtained from generated models. It is evident that an *R-squared* close to 1 reflects an exact linear relationship between predictions and observations. For this function fitting problem, reasonably good predictions were obtained for all datasets.

Table 4- Performance measures of developed ANN models

ANN Model	Samples	mse	R^2
Faulting	**Training**	1.64532e-3	9.98924e-1
	Validation	1.85187e-3	9.98875e-1
	Testing	2.43903e-3	9.98394e-1
Cracking	**Training**	1.36416e-2	9.96456e-1
	Validation	3.18881e-2	9.91453e-1
	Testing	2.99477e-2	9.90665e-1

Also, Figures 5 and 6 display the ANN-predicted distresses against the target counterparts and provide an overall view of the model's accuracy. Obviously, in case of a perfect fitting model, generated outputs and observed data should lie close to 45-degree line. The dashed line in the figures represents the ideal and desired fit line, however the solid line indicates the best fit linear regression line between outputs and targets.

Based on conducted theoretical case studies on a relatively wide range of possible inputs, a reasonable estimation of climate change effects on JPCP performance was achieved via training ANN models. Potentially, adopting these models and developing similar ones under different circumstances can help in determining the range of climate change effects. Overall, given the complexity of climate change and its broad impacts on JPCP service life, the proposed method is deemed useful to facilitate adaptation and planning strategies.

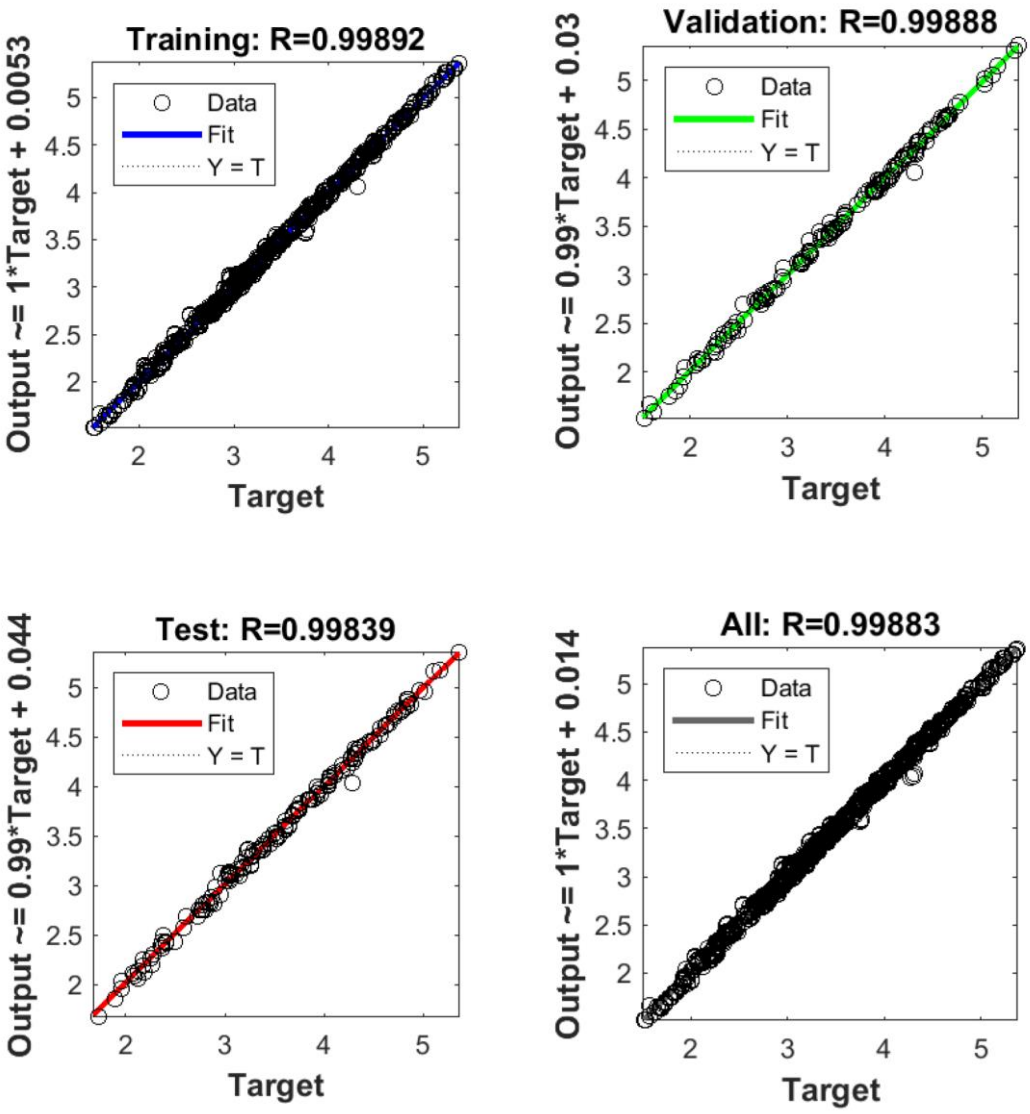

Figure 5- Regression plots of developed ANN model for faulting distress

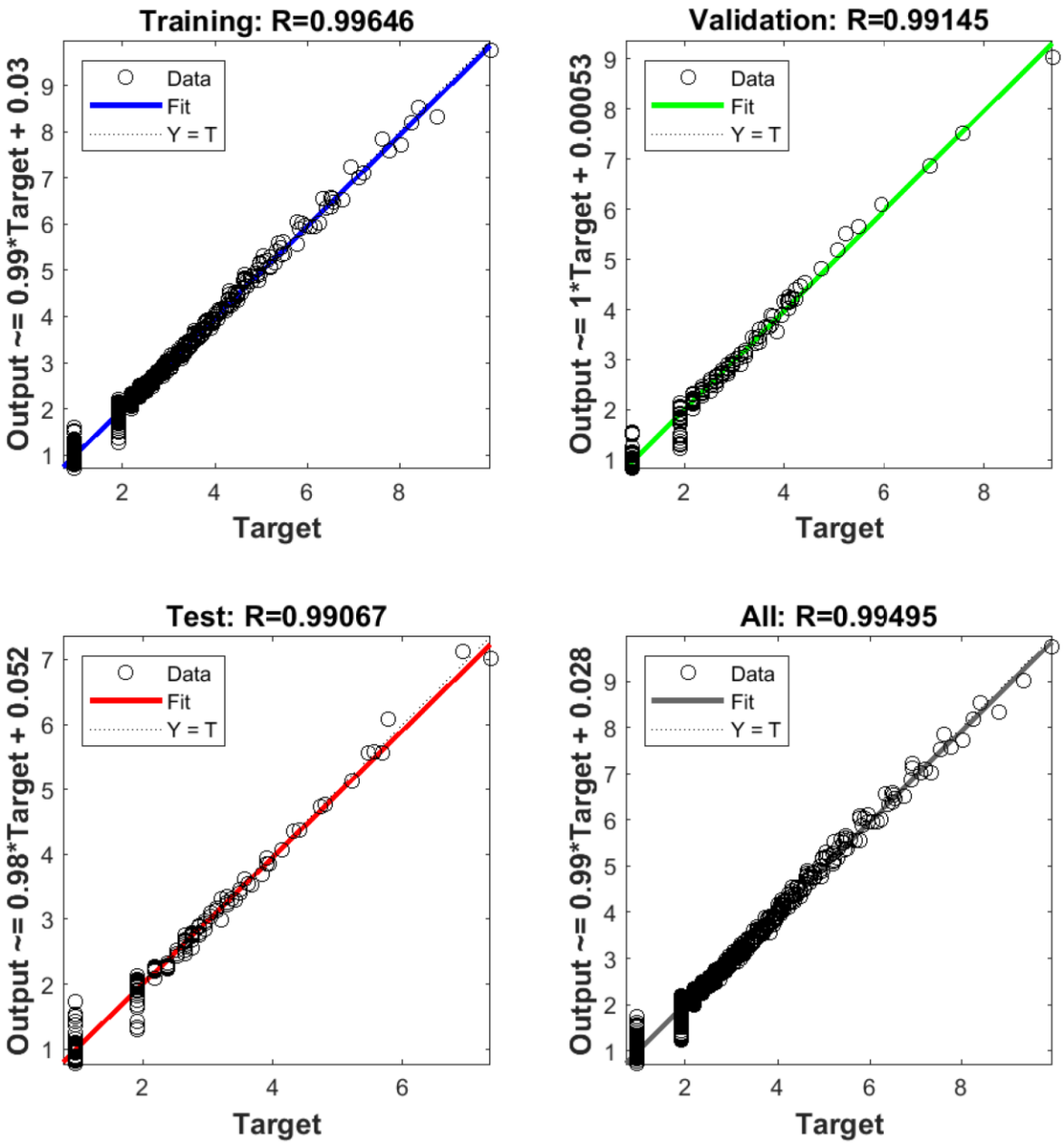

Figure 6- Regression plots of developed ANN model for cracking distress

Conclusions

Many aspects of JPCP infrastructures are directly influenced by climate variability and change. Therefore, it is important to consider physically plausible future climatic conditions in order to assess the impacts of a changing climate and plan adaptation measures. In this study, 972 cases of JPCP structures were simulated using AASHTOWare PMED by including projected climate change for City of Winnipeg, Manitoba. Results of this study showed that joint faulting and slab cracking distresses are likely to be impacted by climate change further in the future. In addition, using a two-layer feed-forward network, promising prediction models were developed for both joint faulting and slab cracking. In summary, proposed method allows for reasonable prediction of JPCP performance under the complex effects of climate change. Finally, using this approach can help in adapting JPCP design to climate change in order to build resilience for public road infrastructures and assets in Canada.

Acknowledgement

This study was undertaken as part of the NRC's Climate Resilient Buildings and Core Public Infrastructure (CRBCPI) initiative and was made possible through funding from Infrastructure Canada under the Pan Canadian Framework on Clean Growth and Climate Change.

REFERENCES

1. ARA Inc., 2004. Guide for mechanistic-empirical design of new and rehabilitated pavement structures, Champaign, Illinois, United States.
2. Nassiri, S., 2011. Establishing permanent curl/warp temperature gradient in jointed plain concrete pavements (Doctoral dissertation, University of Pittsburgh).
3. Qiao, Y., Zhang, Y., Elshaer, M. and Daniel, J.S., 2017. A method to assess climate change induced damage on flexible pavements with machine learning. In Bearing Capacity of Roads, Railways and Airfields (pp. 2103-2109). CRC Press.
4. Mahpour, A. and El-Diraby, T., 2021. Incorporating Climate Change in Pavement Maintenance Policies: Application to Temperature Rise in the Isfahan County, Iran. Sustainable Cities and Society, 71, p.102960.
5. Renard, S., Corbett, B. and Swei, O., 2021. Minimizing the global warming impact of pavement infrastructure through reinforcement learning. Resources, Conservation and Recycling, 167, p.105240.
6. Scinocca, J.F., Kharin, V.V., Jiao, Y., Qian, M.W., Lazare, M., Solheim, L., Flato, G.M., Biner, S., Desgagne, M. and Dugas, B., 2016. Coordinated global and regional climate modeling. *Journal of Climate*, *29*(1), pp.17-35.
7. MTO MERO. 2019. Ontario's Default Parameters for AASHTOWare Pavement ME Design Interim Report.
8. Beale, M., Hagan, M. and Demuth, H., 2019. MATLAB Deep Learning Toolbox™ User's Guide: PDF Documentation for Release R2019a. The MathWorks, Inc.